2021 43rd Annual International Conference of the
IEEE Engineering in Medicine & Biology Society (EMBC)
Oct 31 - Nov 4, 2021. Virtual Conference

On the accuracy of Tier 4 simulations to predict RF heating of wire implants during magnetic resonance imaging at 1.5 T

Pia Sanpitak, Bhumi Bhusal, Bach T. Nguyen, Jasmine Vu, Kelvin Chow, Xiaoming Bi, and Laleh Golestanirad, *Member, IEEE*

***Abstract*— Magnetic Resonance Imaging (MRI) access remains conditional to patients with conductive medical implants, as RF heating generated around the implant during scanning may cause tissue burns. Experiments have been traditionally used to assess this heating, but they are time-consuming and expensive, and in many cases cannot faithfully replicate the *in-vivo* scenario. Alternatively, ISO TS 10974 outlines a four-tier RF heating assessment approach based on a combination of experiments and full-wave electromagnetic (EM) simulations with varying degrees of complexity. From these, Tier 4 approach relies entirely on EM simulations. There are, however, very few studies validating such numerical models against direct thermal measurements. In this work, we evaluated the agreement between simulated and measured RF heating around wire implants during RF exposure at 63.6 MHz (proton imaging at 1.5 T). Heating was assessed around wire implants with 25 unique trajectories within an ASTM phantom. The root mean square percentage error (RMSPE) of simulated vs. measured RF heating remained <1.6% despite the wide range of observed heating (0.2 ℃-53 ℃). Our results suggest that good agreement can be achieved between experiments and simulations as long as important experimental features such as characteristics of the MRI RF coil, implant's geometry, position, and trajectory, as well as electric and thermal properties of gel are closely mimicked in simulations.**

***Clinical Relevance*— This work validates the application of full-wave EM simulations for modeling and predicting RF heating of conductive wires in an MRI environment, providing researchers with a validated tool to assess MRI safety in patients with implants.**

I. Introduction

More than 12 million people in the USA are presently carrying a form of conductive medical implant, such as a cardiac pacemaker or a neuromodulation device. More than 75% of these patients will need magnetic resonance imaging (MRI) exams during their lifetime. Unfortunately, application of MRI is highly limited for these patients due to risk of radiofrequency (RF) heating of the tissue surrounding the implant. This phenomenon, generally known as the “antenna effect”, takes place when the electric field of MRI scanner couples with the metallic leads of the medical device and amplifies the specific absorption rate (SAR) of radiofrequency energy in the tissue, potentially causing tissue burns [1]. Substantial effort has been dedicated to assess RF heating of elongated implants using a combination of full-wave electromagnetic (EM) simulations and phantom experiments [2–10]. Specifically, ISO TS 10974 technical specification describes a four-tier approach for evaluation of MRI-induced RF heating in which the last two tiers (Tier 3 and Tier 4) are applicable to electrically long wire implants (e.g., leads with length comparable to MRI resonance wavelength in the tissue). Tier 3 evaluates the lead's transfer function—the RF heating response of the lead when exposed to a uniform and controlled electric field— and uses it to estimate MRI-induced RF heating when the lead is exposed to any arbitrary incident electric field encountered *in vivo* [11]. Tier 3 approach may yield a large level of overestimation but entails less extensive simulation efforts as the lead's transfer function can be evaluated experimentally or through reduced-size simulations [12,13]. Tier 4 approach, which is based entirely on simulations, reduces uncertainty but requires the accurate quantification of implant's geometry and trajectory, as well as characteristics of MRI environment.

To date, the majority of publications on RF heating of wire-type implants during MRI have used a Tier 3 approach. To our knowledge, there is very little data available on the accuracy of a Tier 4 approach to estimate MRI-induced RF heating of implanted leads [14]. In this work, we performed EM simulations to estimate the local SAR at tips of wire implants with various lengths and trajectories implanted in different locations inside an ASTM-type gel phantom during RF exposure at 63.6 MHz (proton MRI at 1.5 T). We used the calculated SAR in subsequent thermal simulations to predict the temperature rise in the tissue-mimicking gel at the end of 254 seconds RF exposure. We then performed experiments that matched the simulated scenarios to the best of our abilities, mimicking phantom shape and composition; wire length, trajectory, position and material; as well as MRI RF coil and imaging landmark. A total of 25 unique wire trajectories were studied. From these, 6 trajectories were used to create a calibration curve which fitted the experimentally measured RF heating, ΔT_{exp}, to the simulated temperature rise ΔT_{sim}. This curve was then used to predict the ΔT_{exp} from ΔT_{sim} for the remaining 19 trajectories. We found a good fit during the calibration phase (R^2 = 0.96), and the calibrated model predicted the experimental RF heating with high accuracy (root mean square percent error <1.6%).

*Research supported by National Institute of Health grants R03EB029587 and R00EB021320.

Pia Sanpitak and J. Vu are with the Department of Biomedical Engineering, Northwestern University, Evanston, IL, 60608 USA and the Department of Radiology, Northwestern University Chicago, IL 60611 USA.

B. Bhusal and B.T. Nguyen are with the Department of Radiology, Northwestern University Chicago, IL 60611 USA.

K. Chow and X. Bi are with Siemens Healthineers, Malvern, PA, 19355.

Corresponding Author: L. Golestanirad is with the Department of Radiology and Department of Biomedical Engineering, Northwestern University, Chicago, IL, 60611 USA. Email: laleh.rad1@northwestern.edu

Future work will extend the analysis to 3 T and expand to identify and reduce systematic sources of uncertainty.

II. Methods

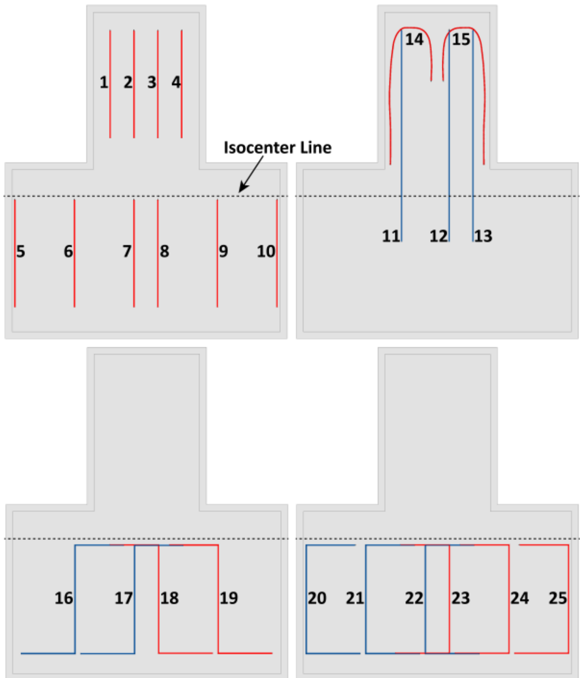

Figure 1. Schematic of different trajectories used for the RF heating measurements.

A. Implant Trajectories

It is well established that the length, trajectory, and orientation of an elongated implant with respect to MRI electric field substantially affects its RF heating [15–18]. In order to assess accuracy of simulations for a wide range of RF heating, we created 25 unique trajectories from 20 cm and 40 cm wires, spanning a large cross section of an ASTM-type phantom. Wires were implanted in locations analogous to phantom's head mimicking deep brain stimulation lead trajectories as well as torso mimicking cardiac lead trajectories (Figure 1). These wire lengths and trajectories are shown to produce a wide range of RF heating in previous studies [15, 19].

B. Experiments

Temperature measurements were performed in a 1.5 T Siemens Aera scanner (Siemens Healthcare, Erlangen, Germany) using an acrylic phantom which was designed based on ASTM recommendations for MRI safety assessment [20]. Rectangular grids and holding posts were designed and used to secure wires at precisely described positions inside the phantom that mimicked simulations. The phantom was filled to a depth of 10 cm with polyacrylamide (PAA) with a conductivity of $\sigma = 0.48$ S/m, and permittivity of $\varepsilon_r = 91.8$, representative of biological tissue. Each trajectory was formed with insulated copper wires (conductor diameter = 1 mm, insulation diameter = 2.5 mm), with a 2 mm exposed tip on one end. Fluoroptic temperature probes (OSENSA, BC, Canada) were attached to the exposed tips to measure the temperature (Figure 2). The phantom was positioned inside the MRI body coil such that a location analogous to the shoulder was at the coil's iso-center. RF exposure was performed using a T_1-weighted turbo spin echo sequence (TE= 7.3 ms, TR = 814.00 ms, flip angle = 150°, B_1^+ RMS= 4.13 μT) for a total of 254 seconds.

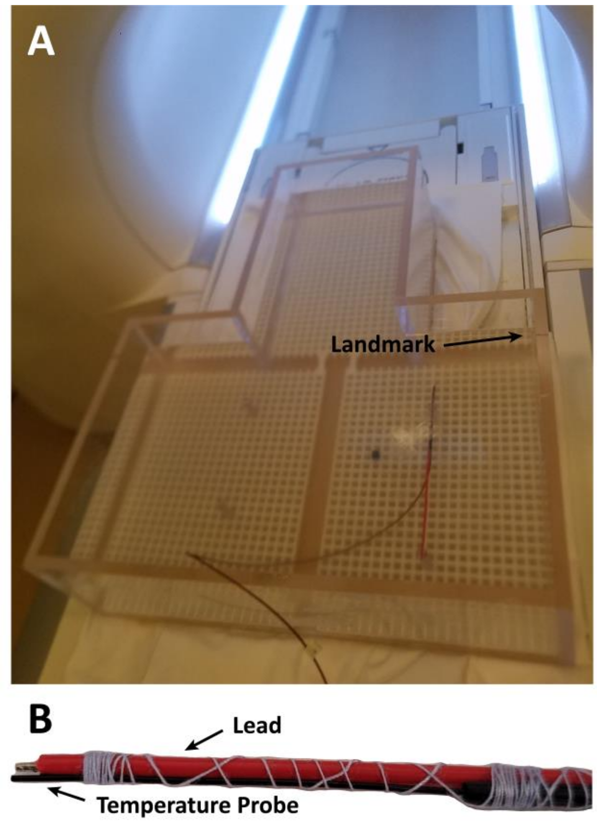

Figure 2. (A) PAA filled phantom with wire and probes in the 1.5 T Aera Scanner. (B) Close up of fluoroptic probe attached to the tip of the generic wire for temperature measurements.

C. Simulations

Electromagnetic simulations were performed using ANSYS Electronic Desktop 2019 R2 (ANSYS, Canonsburg, PA). Wires were modeled as copper ($\sigma = 5.8 \times 10^7$ S/m, diameter = 1 mm) in a urethane insulation ($\sigma = 0$ S/m, $\varepsilon_r = 3.5$, diameter = 2.5 mm) placed inside an acrylic phantom ($\sigma = 0$ S/m, $\varepsilon_r = 3.2$) filled with PAA ($\sigma = 0.48$ S/m, $\varepsilon_r = 91.8$, depth = 10 cm). To enhance simulation accuracy in the locations of predicted SAR hot spots, a 1 cm^3 cubic area of high mesh resolution (rms mesh length = 1.13 mm) was created around the exposed tip of the lead. The RF body coil was modeled as a high-pass 16-rung birdcage coil tuned to 63.6 MHz using a combination of finite element simulations and circuit analysis described in previous works [21, 22]. The detailed geometry of the RF coil was provided by the vendor and replicated in simulations. The coil was excited through two ports separated by 90° on the top end ring (Figure 3). The input power of the coil was adjusted such that it generated the mean $B_1^+ = 4.13$ μT on a transverse plane passing through the center of phantom.

The temperature increase due to RF exposure was calculated using the transient thermal solver of ANSYS Mechanical, which solved Pennes' bio heat equation without perfusion [23]. Thermal properties of PAA which were used

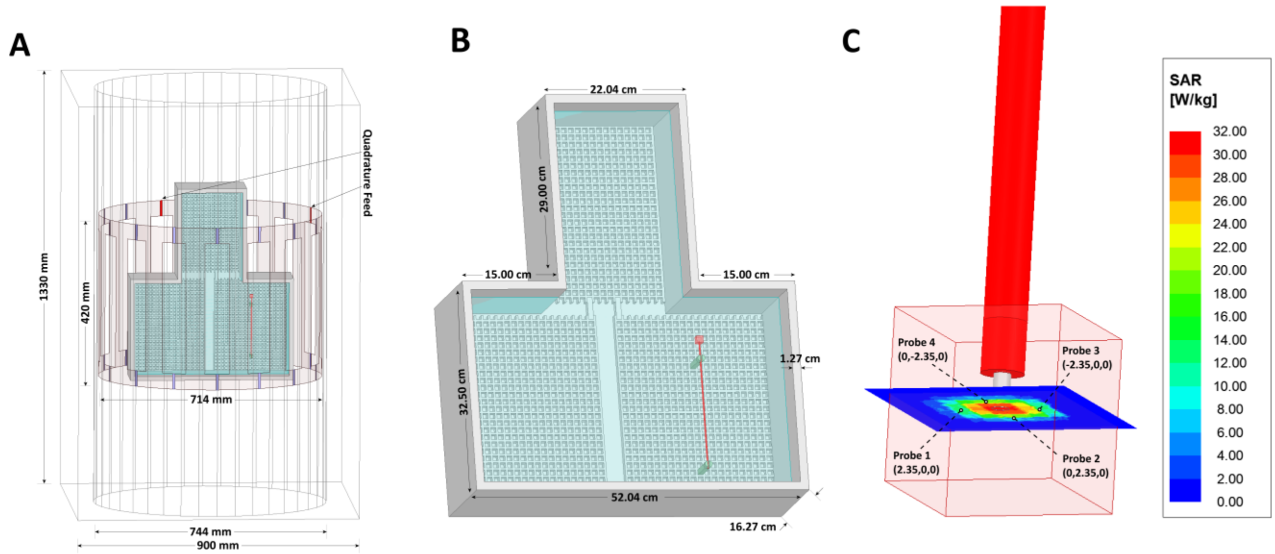

Figure 3. (A) Electromagnetic simulation setup of Trajectory 9 implanted in an acrylic phantom exposed to the RF field from an RF birdcage body coil. (B) Acrylic phantom dimensions. (C) Probe placement and SAR profile occurring in PAA surrounding the tip of the wire for Trajectory 9.

in simulations included density = 1200 kg/m^3, isotropic thermal conductivity = 0.5 Wm^{-1}k^{-1}, and specific heat = 4150 Jkg^{-1}°C^{-1} at 21 °C, that increases with a slope of 2.35 Jkg^{-1}°C^{-2} from 20 °C to 40 °C [19]. The average of the temperature increase at 4 locations (2.35 mm radially from, and 0 mm above the center of the exposed tip) was recorded to more accurately represent the measurements conducted by the fluoroptic temperature probes. The maximum temperature rise after 254 seconds of continuous RF exposure was recorded, calibrated, and compared with experimental results .

III. Results

To account for uncertainties in determination of effective B_1^+, we first created a calibration curve which fitted the simulation results to the experimental results through linear regression using 6 representative trajectories. This resulted in a calibration equation of $\Delta\tilde{T}_{exp}$= 1.0680ΔT_{sim} + 0.5868 with R^2 = 0.96, where $\Delta\tilde{T}_{exp}$ is the predicted change in experimental temperature, and ΔT_{sim} is the change in temperature obtained from the numerical simulations (Figure 4A). We then predicted the experimental temperature rise $\Delta\tilde{T}_{exp}$ for the remaining nineteen trajectories using this calibration curve and calculated the root mean square percentage error as $RMSPE = 100 \times \left(\frac{1}{N}\sum\left[\left(\Delta T_{exp} - \Delta\tilde{T}_{exp}\right)/\Delta T_{exp}\right]^2\right)^{1/2}$ where ΔT_{exp} is the experimentally measured temperature rise and $\Delta\tilde{T}_{exp}$ is the experimental temperature rise predicted by the calibration curve. Even with a large range of temperatures (0.2 °C to 53 °C), we found the RMSPE to remain relatively low at 1.6% (Figure 4B).

IV. Discussion And Conclusion

In recent years, EM simulations have been used alongside experiments to better understand the phenomenology of RF heating of elongated implants in MRI environment. Although simulations have been successfully applied to predict trends of RF heating, that is, to predict if certain changes in implant's characteristics increase or decrease its heating [22], their application to predict the absolute temperature rise in the tissue has proved to be challenging. As such, this study validates that numerical simulations can accurately predict the RF heating of wires for a wide range of trajectories and corresponding temperatures. A greater understanding of RF-induced heating is necessary to advance the field for both better MR-conditional implants and improved imaging methodologies. As experimental determination of optimized imaging parameters and implant characteristics is a lengthy process, the use of validated simulations is highly beneficial to shorten this process.

Our future work includes expanding this work to 3 T and assessing other lead topologies such as helical wires.

References

[1] A. R. Rezai et al., "Neurostimulation System Used for Deep Brain Stimulation (DBS): MR Safety Issues and Implications of Failing to Follow Safety Recommendations," Invest. Radiol., vol. 39, no. 5, pp. 300–303, 2004.

[2] C. E. McElcheran, B. Yang, K. J. Anderson, L. Golestanirad, and S. J. Graham, "Parallel radiofrequency transmission at 3 tesla to improve safety in bilateral implanted wires in a heterogeneous model," Magnetic resonance in medicine, vol. 78, no. 6, pp. 2406-2415, 2017.

[3] L. Golestanirad et al., "Reconfigurable MRI coil technology can substantially reduce RF heating of deep brain stimulation implants: First in-vitro study of RF heating reduction in bilateral DBS leads at 1.5 T," PloS one, vol. 14, no. 8, 2019.

[4] L. Golestanirad et al., "Changes in the specific absorption rate (SAR) of radiofrequency energy in patients with retained cardiac leads during MRI at 1.5 T and 3T," Magnetic resonance in medicine, vol. 81, no. 1, pp. 653-669, 2019.E. H. Miller, "A note on reflector arrays (Periodical style—Accepted for publication)," IEEE Trans. Antennas Propagat., to be published.

[5] E. Kazemivalipour et al., "Reconfigurable MRI technology for low-SAR imaging of deep brain stimulation at 3T: Application in bilateral leads, fully-implanted systems, and surgically modified lead trajectories," NeuroImage, vol. 199, pp. 18-29, 2019.

[6] C. McElcheran et al., "Numerical simulations of realistic lead trajectories and an experimental verification support the efficacy of parallel radiofrequency transmission to reduce heating of deep brain stimulation implants during MRI," Scientific reports, vol. 9, no. 1, pp.

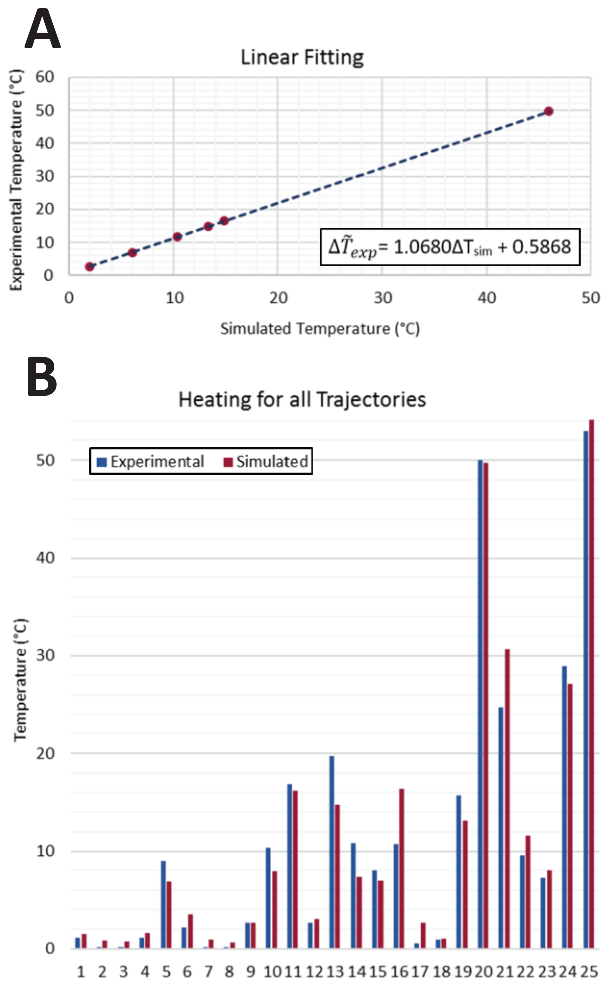

Figure 4. (A) Calibration curve fitting simulation results to experimental results. (B) Plots of temperature increase for different trajectories.

1-14, 2019.M. Young, The Techincal Writers Handbook. Mill Valley, CA: University Science, 1989.

[7] B. Bhusal et al., "Effect of device configuration and patient's body composition on the RF heating and non-susceptibility artifact of deep brain stimulation implants during MRI at 1.5 T and 3 T," Journal of Magnetic Resonance Imaging vol. (In Press), 2020.

[8] L. Golestanirad et al., "RF heating of deep brain stimulation implants in open-bore vertical MRI systems: A simulation study with realistic device configurations," Magnetic resonance in medicine, vol. 86, no. 6, pp. 2284-92, 2020.

[9] E. Kazemivalipour et al., "RF heating of deep brain stimulation implants during MRI in 1.2 T vertical scanners versus 1.5 T horizontal systems: A simulation study with realistic lead configurations," in 2020 42nd Annual International Conference of the IEEE Engineering in Medicine & Biology Society (EMBC), 2020: IEEE, pp. 6143-6146

[10] B. Bhusal, B. Keil, J. Rosenow, E. Kazemivalipour, and L. Golestanirad, "Patient's body composition can significantly affect RF power deposition in the tissue around DBS implants: ramifications for lead management strategies and MRI field-shaping techniques," Physics in Medicine & Biology, vol. 66, no. 1, p. 015008, 2021.

[11] ISO TS 10974: Assessment of the safety of magnetic resonance imaging for patients with an active implantable medical device, Geneva, Switzerland, 2018.

[12] S. Feng, R. Qiang, W. Kainz, and J. Chen, "A technique to evaluate MRI-induced electric fields at the ends of practical implanted lead," IEEE Transactions on Microwave Theory and Techniques, vol. 63, no. 1, pp. 305-313, 2014.

[13] A. Missoffe and S. Aissani, "Experimental setup for transfer function measurement to assess RF heating of medical leads in MRI: Validation in the case of a single wire," Magnetic resonance in medicine, vol. 79, no. 3, pp. 1766-1772, 2018.

[14] E. Cabot, E. Zastrow, and N. Kuster, "Safety assessment of AIMDs under MRI exposure: Tier3 vs. Tier4 evaluation of local RF-induced heating," in 2014 International Symposium on Electromagnetic Compatibility, Tokyo, 2014: IEEE, pp. 237-240.

[15] E. Mattei et al., "Complexity of MRI induced heating on metallic leads: experimental measurements of 374 configurations," Biomedical engineering online, vol. 7, no. 1, p. 11, 2008.

[16] L. Golestanirad, L. M. Angelone, M. I. Iacono, H. Katnani, L. L. Wald, and G. Bonmassar, "Local SAR near deep brain stimulation (DBS) electrodes at 64 and 127 MH z: A simulation study of the effect of extracranial loops," Magnetic resonance in medicine, vol. 78, no. 4, pp. 1558-1565, 2017.

[17] L. Golestanirad, B. Keil, L. M. Angelone, G. Bonmassar, A. Mareyam, and L. L. Wald, "Feasibility of using linearly polarized rotating birdcage transmitters and close-fitting receive arrays in MRI to reduce SAR in the vicinity of deep brain simulation implants," Magnetic resonance in medicine, vol. 77, no. 4, pp. 1701-1712, 2017.

[18] L. Golestanirad et al., "RF-induced heating in tissue near bilateral DBS implants during MRI at 1.5 T and 3T: The role of surgical lead management," NeuroImage, vol. 184, pp. 566-576, 2019.

[19] P. Nordbeck et al., "Measuring RF-induced currents inside implants: Impact of device configuration on MRI safety of cardiac pacemaker leads," Magnetic resonance in medicine, vol. 61, no. 3, pp. 570-578, 2009.

[20] F04 Committee, "Test Method for Measurement of Radio Frequency Induced Heating On or Near Passive Implants During Magnetic Resonance Imaging," ASTM International.

[21] L. I. Navarro de Lara, L. Golestanirad, S. N. Makarov, J. P. Stockmann, L. L. Wald, and A. Nummenmaa, "Evaluation of RF interactions between a 3T birdcage transmit coil and transcranial magnetic stimulation coils using a realistically shaped head phantom," Magnetic Resonance in Medicine, vol. 84, no. 2, pp. 1061-1075, 2020.

[22] B. T. Nguyen, J. Pilitsis, and L. Golestanirad, "The effect of simulation strategies on prediction of power deposition in the tissue around electronic implants during magnetic resonance imaging," Physics in Medicine & Biology, vol. 65, no. 18, p. 185007, 2020.

[23] L. Golestanirad et al., "Reducing RF-induced heating near implanted leads through high-dielectric capacitive bleeding of current (CBLOC)," IEEE transactions on microwave theory and techniques, vol. 67, no. 3, pp. 1265-1273, 2019.